J Mol Model (2004) 10:25–31
DOI 10.1007/s00894-003-0165-6

ORIGINAL PAPER

Bruno Rizzuti · Marcel Swart · Luigi Sportelli · Rita Guzzi

Active site modeling in copper azurin molecular dynamics simulations

Received: 25 February 2003 / Accepted: 22 September 2003 / Published online: 23 December 2003

Abstract Active site modeling in molecular dynamics simulations is investigated for the reduced state of copper azurin. Five simulation runs (5 ns each) were performed at room temperature to study the consequences of a mixed electrostatic/constrained modeling for the coordination between the metal and the polypeptide chain, using for the ligand residues a set of charges that is modified with respect to the apo form of the protein by the presence of the copper ion.

The results show that the different charge values do not lead to relevant effects on the geometry of the active site of the protein, as long as bond distance constraints are used for all the five ligand atoms. The distance constraint on the O atom of Gly45 can be removed without altering the active site geometry. The coordination between Cu and the other axial ligand Met121 is outlined as being flexible. Differences are found between the bonds of the copper ion with the two apparently equivalent $N^{\delta 1}$ atoms of His46 and His117.

The overall findings are discussed in connection with the issue of determining a model for the active site of azurin suitable to be used in molecular dynamics simulations under unfolding conditions.

B. Rizzuti · L. Sportelli · R. Guzzi (✉)
Dipartimento di Fisica and Unità INFM,
Laboratorio di Biofisica Molecolare,
Università della Calabria, Ponte P. Bucci,
Cubo 30C, 87030 Rende CS, Italy
e-mail: guzzi@fis.unical.it
Tel.: +39-0984-496077
Fax: +39-0984-494401

M. Swart
Theoretische Chemie (MSC),
Rijksuniversiteit Groningen,
Nijenborgh 4, 9747 AG Groningen, The Netherlands

Present address:
M. Swart, Organische en Anorganische Chemie,
Vrije Universiteit Amsterdam,
De Boelelaan 1083, 1081 HV Amsterdam, The Netherlands

Keywords Azurin · Active site · Molecular dynamics simulation

Introduction

Azurin is a blue copper protein belonging to the cupredoxins family, acting as an electron transfer shuttle in the redox system of *Pseudomonas aeruginosa* and other bacteria. A copper (Cu) ion is sandwiched between two β-sheets (Fig. 1), about 0.7 nm below the protein surface, coordinated in a trigonal bipyramidal geometry to five atoms, three equatorial ($N^{\delta 1}{}_{His46}$, S_{Cys112} and $N^{\delta 1}{}_{His117}$) and two axial (O_{Gly45} and S_{Met121}). Modeling the active site is an important issue in molecular dynamics simulations (MDS) of metal proteins. Different parameterizations of a Cu ion bound to a protein have been proposed during the last decade, [1, 2, 3, 4, 5, 6, 7, 8, 9] most of them obtained by less appropriate methods. Therefore, a simple model based on experimental evidences [10] describes each Cu–ligand interaction by covalent bonds in room temperature MDS of cupredoxins.

The presence of the Cu ion in the active site is expected to alter the charge distribution on all of the atoms in the ligand residues with respect to the apo form of azurin, hence modifying the electrostatic interactions within this region. An experimental determination of the charge value of every single atom of the ligand residues is not possible, as atomic charges are not observables of the wavefunction. However, the consequences of the alteration of the charges are generally assumed to be negligible in nanoseconds MDS of native azurin [11, 12] because of the use of distance constraints on the Cu–ligand bonds. This assumption justifies the use of a set of charges that are unmodified by the presence of the Cu ion: charge values are uniquely determined by the simulated pH, in the active site as well as in all of the other regions of the protein.

However, the above-mentioned assumption needs to be tested. In fact, even if every Cu–ligand bond distance is constrained, no bond angle involving the Cu ion is usually

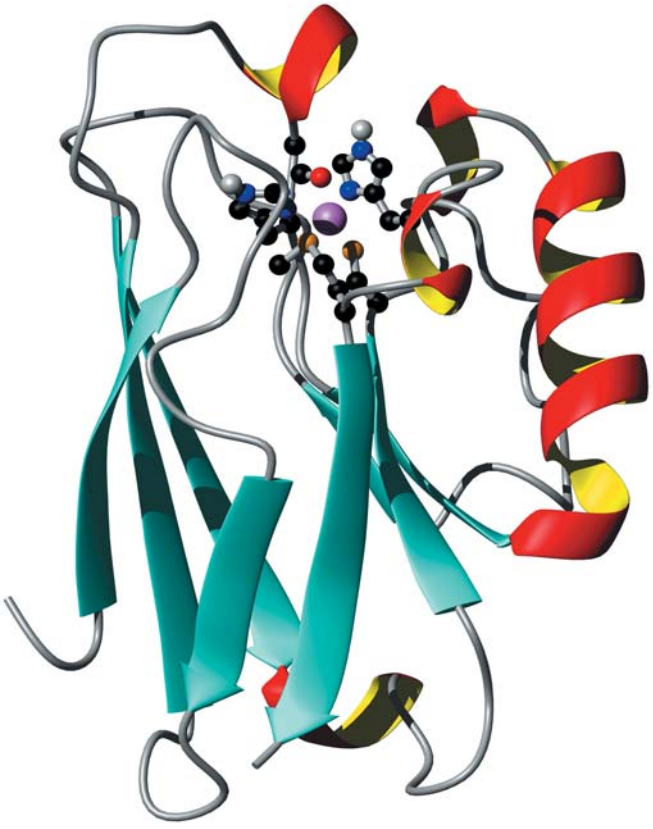

Fig. 1 Standard ribbon representation of azurin: active site is on top and the α-helix on the right (with N-terminus on bottom and C-terminus on top). Active site atoms are explicitly shown, including the copper ion (in *violet*)

defined in MDS of azurin. [12, 13] In principle, this means that an alteration of the electrostatic field in the active site could lead to alterations in its geometry. Furthermore, the modification of the charge distribution around the Cu atom could influence the behavior of other protein regions, eventually reflecting in some feedback effects also on the active site itself.

In addition, the use of constraints on all of the five Cu–ligand distances may not be appropriate for simulations under unfolding conditions, for instance at high temperature. In fact, recent studies suggest that, in the unfolded state of azurin, the metal ion is coordinated by a lower number of ligands, [14] possibly only three. [15] In this respect, it is worth exploring different possibilities of modeling the active site of azurin. In particular, it is interesting to test whether the electrostatic interactions between the Cu ion and the ligands, which are *de facto* neglected in the presence of constraints, could be sufficient to maintain the native coordination of the metal at room temperature and also useful to describe the experimental findings at higher temperature or under other extreme conditions. This would allow us to remove some of the constraints between the Cu and its ligand atoms, therefore constituting a better reference model for unfolding simulations of azurin.

These aspects are explored in this work, where the consequences of adopting an ionic modeling for the reduced state of the active site of azurin in MDS are investigated. The starting point is the result recently obtained by Density Functional Theory, [16] showing that a set of charges that takes into account the presence of the Cu ion in the active site (named DFT hereafter), different from the one currently used (named GROMOS) that is independent upon the presence of the metal, is able to reproduce more accurately the ionization potential of azurin. DFT charges results from high-level Density Functional Theory calculations [16] performed with the ADF program [17] using the Becke–Perdew XC-potential in a large basis set, and will be presented elsewhere in more detail. [18] In this paper, we discuss first of all the consequences of adopting in MDS either the set of charges DFT or GROMOS when bond distance constraints are used. Secondly, adopting the DFT set of charges, we present the effects of different simulations where the systematic removal of two Cu–ligand constraints is performed. In one case the removal of the axial ligand constraints (Gly45 and Met121), whose interactions with the metal are supposed to be wholly or partly Coulombic in character, [19] is considered. Then the removal of the Cu–O_{Gly45} bond distance constraint is coupled to either Cu–N_{His46} or Cu–N_{His117}, according to recent experimental studies suggesting that Met121 is still bound to the Cu ion in the unfolded state of azurin, whereas one of the two His ligands, [15] possibly His46, [20, 21] may be lost.

The results show that using the two different set of charges does not lead to any relevant effect on the active site geometry, as long as bond distance constraints are used for the five ligand atoms. The removal of the constraints on the two axial ligands is sufficient to maintain Gly45 in the proper geometry within the 5-ns simulation time, but the coordination between Cu–S_{Met121} is lost. Bond distance constraints are mandatory to preserve the His117 ligand, and the Cu–O_{Gly45}/Cu–N_{His46} distances are also difficult to be simultaneously maintained by using purely electrostatic interactions.

Computational methods

Simulations were performed using the GROMACS package [22, 23] with the GROMOS96 force field 43A1, [24] which employs a united-atom model with hydrogens on aliphatic carbons subsumed in an increased van der Waals radius of C atoms. The starting structure of the protein was modeled from the 4AZU entry of the Protein Data Bank, [25] containing the X-ray coordinates of *Pseudomonas aeruginosa* azurin resolved at 0.19 nm in a tetramer unit. [26, 27] Only one monomer was considered, together with 80 related crystallization waters. The protonation state of the protein was adjusted in order to mimic a pH value of 7.0. All Lys residues were positively charged, and His residues were modeled as neutral by protonating the $N^{\varepsilon 2}$ atom. In the active site, for the

Cys112 ligand residue the deprotonated model was used. No angle and dihedral restraints were used for the Cu ion, and bond lengths with the ligand atoms were fixed at their crystal values [27] when constraints were employed. The simulations were carried out in a periodic box with a rhombic dodecahedron shape. The system formed by the protein and the crystallization waters was placed at a minimum distance of 0.8 nm with respect to the box walls and additionally hydrated. The box volume was 184.19 nm^3 and the resulting number of solvent molecules was 5,441, corresponding to 6.8 g water/g protein. All the water molecules were represented with the simple point charge (SPC) model. [28]

For the evaluation of the nonbonded interactions, a twin range cutoff of 8.0 and 1.4 nm was used, with an update of the neighbors pair list every five steps. The time step for the simulations was 2 fs. The LINCS [29] and SETTLE [30] algorithms were used to constrain, respectively, the bond distances in the protein and the bond distances and angles in the water molecules. To keep the system at constant temperature a Berendsen thermostat was applied, [31] using a coupling time of 0.1 ps. Constant pressure was maintained by coupling to an external bath with a reference value of 10^5 Pa, with a coupling time of 1.0 ps and an isothermal compressibility of 4.6×10^{-10} Pa^{-1}. [31] The system was relaxed by 80 steps of steepest descent minimization, using a force constant of 1,000 kJ mol^{-1} nm^{-2} to restrain the position of the protein atoms in the crystallographic configuration. Initial atomic velocities were assigned from a Maxwellian distribution corresponding to a starting temperature of 250 K. Simulated annealing was performed for 50 ps to gradually increase the temperature up to the final value of 300 K. Simulations were performed for 5 ns, saving the trajectory data every 0.2 ps.

Results and discussion

Five different MDS of 5 ns were performed to investigate the consequences of the modification of the charge distribution in the active site due to the presence of the Cu ion, and of a constrained or unconstrained modeling of the Cu–ligand bond interactions. In the first two simulations the effects of using two different sets of charges (GROMOS and DFT) were compared in the presence of bond distance constraints on all of the five ligands. In the subsequent three MDS, the DFT charge set was always employed and two Cu–ligand distances were left unconstrained. The Cu–O_{Gly45} interaction, which is essentially Coulombic, [10] was left unconstrained in these three MDS and the Cu–S_{Cys112} bond, which on the contrary shows a highly covalent character, [10] was modeled by using a distance constraint. Results are discussed separately, according to the following scheme:

Using distance constraints on all the five ligands:

– Comparison between set of charges GROMOS and DFT

Using the DFT set of charges:

– Electrostatic modeling of Cu–O_{Gly45}/Cu–S_{Met121} interactions (constraints on Cu–N_{His46}/Cu–S_{Cys112}/Cu–N_{His117})
– Electrostatic modeling of Cu–O_{Gly45}/Cu–N_{His117} (constraints on Cu–N_{His46}/Cu–S_{Cys112}/Cu–S_{Met121}) and Cu–O_{Gly45}/Cu–N_{His46} (constraints on Cu–S_{Cys112}/Cu–N_{His117}/Cu–S_{Met121}) interactions

Comparison between set of charges GROMOS and DFT

The sets of charges used in the first two simulations are reported in Table 1. In the first set of values, named GROMOS, atomic charge values correspond to the apo form of the protein at neutral pH, accordingly to the

Table 1 Charge values for azurin active site according to GROMOS (GROMOS96 force field 43A1) [24] and DFT [16, 18] sets. All the charges are in *e* units

Atom name	GROMOS set	DFT set
Gly45		
C	0.00	+0.41
O	−0.38	−0.50
C^{α}	+0.38	+0.13
His46		
N	+0.28	−0.69
H	−0.28	+0.34
C^{α}	0.00	+0.38
C^{β}	0.00	+0.11
C^{γ}	+0.13	+0.06
$N^{\delta1}$	−0.58	−0.41
$C^{\delta2}$	0.00	+0.05
$C^{\varepsilon1}$	+0.26	+0.36
$N^{\varepsilon2}$	0.00	−0.52
$H^{\varepsilon2}$	+0.19	+0.42
Cys112[a]		
C^{α}	0.00	+0.02
C^{β}	−0.10	+0.04
S^{γ}	−0.40	−0.60
His117		
C^{α}	0.00	−0.03
C^{β}	0.00	+0.18
C^{γ}	+0.13	+0.04
$N^{\delta1}$	−0.58	−0.39
$C^{\delta2}$	0.00	+0.05
$C^{\varepsilon1}$	+0.26	+0.40
$N^{\varepsilon2}$	0.00	−0.51
$H^{\varepsilon2}$	+0.19	+0.40
Met121		
C^{α}	0.00	−0.02
C^{β}	0.00	+0.12
C^{γ}	0.00	+0.07
S^{δ}	0.00	−0.26
C^{ε}	0.00	+0.13
Cu		
	+0.50[b]	+0.21

[a] CYS residue in GROMOS96 force field 43A1, [24] deprotonated, total charge −0.5
[b] Assigned to obtain a global null net charge for the active site

GROMOS96 force field 43A1. [24] In particular, for the Cys112 Cu–ligand the standard model of the GROMOS force field of deprotonated cysteine is used, which assigns a −0.50e charge to the overall residue. This charge is compensated by the +0.50*e* charge assigned to the Cu ion. All the other ligand residues are neutral on the whole, the His46 and His117 being both protonated at $N^{\varepsilon 2}$. The other set of charges, named DFT, was modeled on the basis of the Density Functional Theory calculations of Swart et al. [16] The charge distribution was obtained for active site structures that were taken from crystal structures of wild type *Pseudomonas aeruginosa* azurin, where hydrogen atoms were added where appropriate and only their positions were optimized. The complete side chain (the main chain for Gly45) and the C^{α} of the ligand residues were taken into account in these calculations, leading to a total of 61 atoms; further details will be published elsewhere. [18] The charge of the Cu ion is lowered in this case to +0.21*e*, and charge values of all the side chain atoms of the ligand residues are different with respect to the GROMOS set. Bond distances between the Cu ion and the five ligand atoms were constrained in both the simulations.

The geometry of the active site of azurin is negligibly altered with respect to the starting configuration, independently of the charge set used. Differences in the dynamic behavior of the protein are detected by calculating the root mean square fluctuations (RMSF) of the atomic positions of the backbone, after removing the rototranslation of the molecule by means of a mass-weighted least-squares algorithm superimposing the C^{α} atoms onto the reference configuration. Fluctuations are calculated for both the simulations in the time interval 2–5 ns, after 2 ns of equilibration of the protein structure. The RMSF of the main chain (N–C^{α}–CO) atoms are reported in Fig. 2 for MDS using the GROMOS (*red* line) and DFT (*black* line) set of charges, together with the same value derived from the B-factors of the crystallographic structure (*blue* line) of wild type azurin. [27] The RMSF are quantitatively and qualitatively similar in the two simulations. Significant differences are only found in correspondence with His117, which is one of the Cu ligand residues, and with the N-terminus of the unique α-helix of azurin (Fig. 1). In the first case, the different behavior is a direct consequence of the set of charges used. In the latter case, on the contrary, the consequences of altering the charge distribution are indirectly reflected on a region far away from the active site. Whether or not a stabilizing effect could be due to electrostatic interactions related to the presence of the helix dipole is questionable. [32, 33] However, the results obtained using the DFT set of charges in this case (and also for His117) are in a better agreement with the corresponding crystallographic RMSF value. More generally, a good agreement is found between simulated and experimental fluctuations (Fig. 2). Relevant flexibility in both the Lys74–Asp77 and Lys103–Glu106 turns, showing the highest simulated values, is also reported in NMR investigation of wild type azurin in solution. [34]

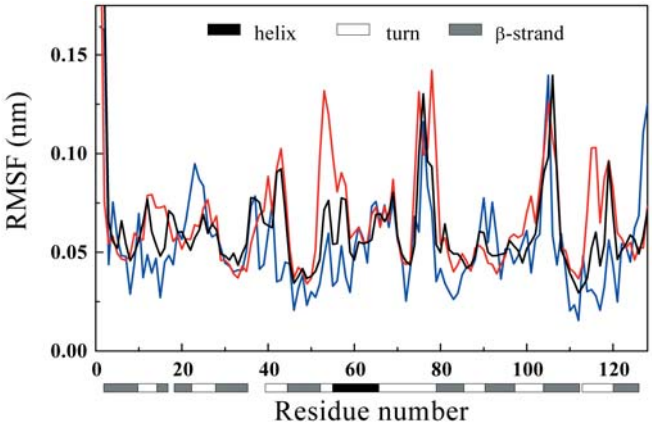

Fig. 2 Positional root mean square fluctuations (RMSF) plotted versus main chain atoms (N–C^{α}–CO) calculated from the simulated structure averaged over the 2–5-ns time interval, using the DFT [16, 18] (*black* line) and GROMOS [24] (*red* line) charge sets. The same values obtained from the crystallographic B-factors [27] (*blue* line) are reported. Secondary structure elements are also shown

Comparative runs performed with the GROMOS and DFT charge sets at lower hydration (minimum distance of the system from the box of 0.7 nm, resulting in 4,880 solvent molecules) confirmed the general behavior discussed above, indicating that the differences observed should be attributed to the charge distribution in the active site.

Electrostatic modeling of $Cu–O_{Gly45}$/$Cu–S_{Met121}$ interactions

The hypothesis of a wholly Coulombic modeling of the interactions between the Cu ion and the two axial ligands was tested by eliminating the bond constraints between both $Cu–O_{Gly45}$ and $Cu–S_{Met121}$. It should be noted that the electrostatic interaction energy between $Cu–O_{Gly45}$ is even lower using the DFT set of charges than using the GROMOS one. In fact, although the O_{Gly45} is more charged (−0.50*e*), the Cu ion has a lower value (+0.21*e*). On the other hand, all the atoms in the side chain of Met are considered neutral in the 43A1 force field, [24] whereas in the DFT set values up to −0.26*e* for S_{Met121} are present. Therefore, electrostatic interactions exist between the Cu ion and the Met121 side chain.

The distances between $Cu–O_{Gly45}$ and $Cu–S_{Met121}$ as a function of time are both reported in Fig. 3. The Gly45 residue maintains a correct geometry, and the $Cu–O_{Gly45}$ distance could be sufficient to consider the ligand coordination preserved. In fact, a value of 0.33±0.03 nm is found, the error on the average value being the standard deviation. Fluctuations are a consequence of the dynamics of the protein, and the simulated distance is consistent with the experimental value of 0.302±0.008 nm for the reduced state of wild type azurin (all the experimental values are obtained averaging over the four monomers in the X-ray unit). [27] In contrast, the distance between Cu

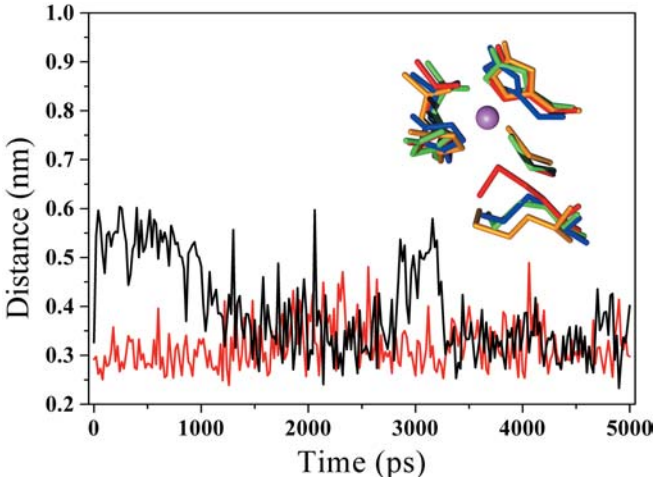

Fig. 3 Distance between Cu–O_{Gly45} (*red* line) and Cu–S_{Met121} (*black* line), as a function of simulation time (sampling time is 20 ps). In the inset, stick representation of azurin active site at different simulation times: starting position (*red*), and after 1,300 ps (*yellow*), 2,060 ps (*green*) and 3,160 ps (*blue*), the latter three corresponding to local maxima of the Cu–S_{Met121} simulated distance

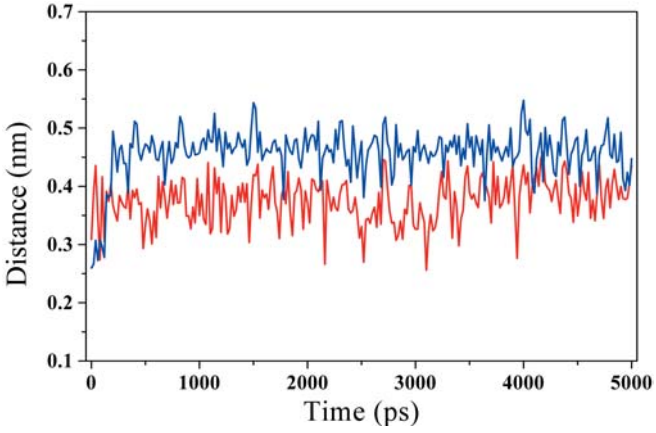

Fig. 4 Distance between Cu–O_{Gly45} (*red* line) and between Cu–N_{His117} (*blue* line), as a function of simulation time (sampling time is 20 ps)

and S_{Met121} is higher than the experimental value, 0.325±0.007 nm. For most of the time electrostatic interactions are sufficient to preserve a correct distance, but in some intervals the dynamics of the Met residue prevails, leading to values around 0.5 nm. In particular, as we show in the inset in Fig. 3, fluctuations of the distance value are mainly due to rotations around the χ angles in the Met side chain rather than to mobility of the main chain. The length of the Cu–S_{Met} bond is suggested to significantly affect the reduction potential within the blue copper proteins family. [35, 36, 37] This hypothesis, which supports the entatic state or induced-rack theory, [38, 39, 40] has been recently challenged by Ryde and coworkers on the basis of quantum chemical calculations. [41, 42, 43] The result obtained in our simulation shows a better agreement with the latter point of view, which excludes a high protein strain exerted by the Cu ion on the Met121 residue. In the absence of a distance constraint, the flexible nature of the coordination between Cu–S_{Met121} becomes evident when observed over the 5 ns time scale. In fact, the Met side chain returns spontaneously and for relatively long periods to its starting position (Fig. 3). This is in agreement with the results obtained by quantum chemical calculations for both azurin [44] and plastocyanin, [9] another member of the cupredoxin family, whose Cu–S_{Met} bonds are described as floppy. A flat potential energy surface for the Met121 residue in azurin is also found in DFT calculations by Swart et al. [18, 45] monitoring the energy needed to move this ligand away from the Cu.

Electrostatic modeling of Cu–O_{Gly45}/Cu–N_{His117} and Cu–O_{Gly45}/Cu–N_{His46} interactions

The possibility that in the unfolded state covalent bonds are present in azurin between the Cu ion and the two S ligands plus only one of the two N_{His} has recently been suggested by experimental studies. [15] For this reason, two MDS were performed eliminating the bond distance constraints between Cu–O_{Gly45} and Cu–N_{His117} in one case, and those between Cu–O_{Gly45} and Cu–N_{His46} in the other.

In the first simulation, the distances between Cu–O_{Gly45} and Cu–N_{His117} as a function of time are reported in Fig. 4. Both the curves rapidly reach a relatively stable value, 0.35±0.04 and 0.45±0.04 nm respectively. Electrostatic interactions are sufficient to maintain the Cu–O_{Gly45} at a distance that, though higher than in the previous simulation, nevertheless remains within the bounds set by the crystallographic value and the experimental uncertainty associated with it. [27] In contrast, the Cu–N_{His117} distance of 0.45±0.04 nm is much higher than the experimental value, 0.210±0.009 nm. As a consequence, the correct Cu–N_{His117} distance in the active site modeling of azurin in MDS might probably not be achieved without using a distance constraint. Modeling by means of a covalent bond is in complete agreement with the experimental data, pointing out that coordination between the Cu ion and the His117 residue is very strong, and most likely conserved even in the unfolded state of azurin. [20, 21]

The Cu–ligand distances obtained in the last simulation, when the distances between Cu–O_{Gly45} and Cu–N_{His46} are both unconstrained, are reported in Fig. 5. Several hundred picoseconds are necessary to reach a dynamic equilibrium. Both the distances, 0.37±0.05 nm for Cu–O_{Gly45} and 0.34±0.05 nm for Cu–N_{His46}, are higher than the crystallographic values, 0.302±0.008 and 0.213±0.009 nm respectively. [27] However, when compared with the previous simulation results, qualitative

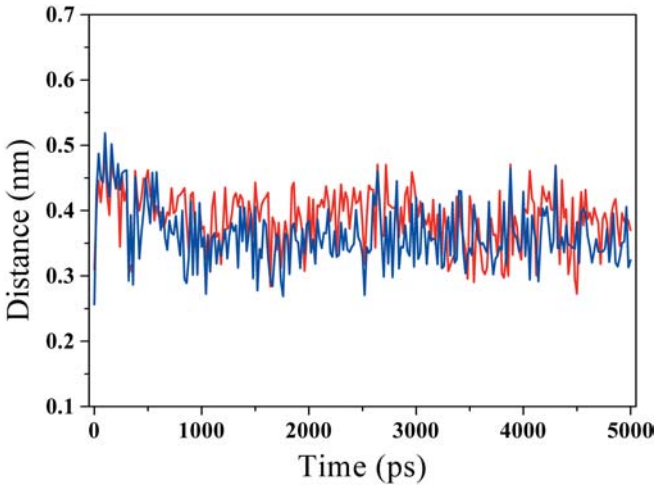

Fig. 5 Distance between Cu–O_{Gly45} (*red* line) and between Cu–N_{His46} (*blue* line), as a function of simulation time (sampling time is 20 ps)

behavior is correctly obtained in this case, the Cu–N_{His46} distance being lower than the Cu–O_{Gly45} one. In addition, it should be remarked that the dynamics of Gly45 and His46 are highly correlated, the two residues being consecutive in the protein sequence. Therefore, an ad hoc tuning of the atomic charge values could be sufficient to adjust the position of both the residues in MDS simultaneously according to the experiments. In this case, avoiding bond distance constraints could constitute a better modeling for the azurin active site to be used in MDS of the (un)folding process. In fact, experimental data suggest that the Cu–N_{His46} bond is weaker than the similar Cu–N_{His117} one, being lost in the unfolded state of azurin. [20, 21]

Conclusions

An accurate modeling of the active site is necessary to describe metal proteins correctly. Metal ions show a high degree of structural variability in the coordination, so that an *ad hoc* parameterization is generally necessary. Furthermore, the presence of the protein matrix should be considered, so that simulations at the atomic level and on a nanosecond time scale are required to take into account the overall dynamics of the macromolecule.

In this work, an ionic model for the Cu^+–ligand interactions was employed to study the active site of reduced azurin in MDS. Electrostatic modeling avoids the necessity to define bond stretching, angle bending and dihedral interactions involving the Cu ion, and allows the dissociation of the Cu–ligand bonds under unfolding conditions.

The results show that using a set of charges for the metal ligand residues that takes the presence of the Cu ion into account, if bond distance constraints are used, does not lead to a relevant effect on the geometry of the active site of the protein. On the other hand, when distance constraints are removed, differences are found between the coordination of Cu ion with the two axial ligands, Gly45 and Met121. Furthermore, a different behavior is registered between the two apparently equivalent ligands His46 and His117. These findings could be of interest in designing a model for the active site of azurin for MDS under unfolding conditions.

Acknowledgements B.R. is grateful to Alan Mark and Alessandra Villa for helpful discussions and hospitality in the Molecular Dynamics group at the Rijksuniversiteit Groningen. Thanks are also due to Regione Calabria for a fellowship and to CNR (Consiglio Nazionale delle Ricerche) for financial support. M.S. thanks NWO/CW and Unilever Research Vlaardingen for their financial support. MOLMOL [46] was used for the protein displays.

References

1. Shen J, Wong CF, Subramanian S, Albright TA, McCammon JA (1990) J Comput Chem 11:346-350
2. Fields BA, Guss JM, Freeman HC (1991) J Mol Biol 222:1053–1065
3. Banci L, Carloni P, La Penna G, Orioli PL (1992) J Am Chem Soc 114:6994–7001
4. Wang CX, Bizzarri AR, Xu YW, Cannistraro S (1994) Chem Phys 183:155–166
5. Mark AE, van Gunsteren WF (1994) J Mol Biol 240:167–176
6. Falconi M, Gallimbeni R, Paci E (1996) J Comput Aided Mol Design 10:490–498
7. Ungar LW, Scherer NF, Voth GA (1997) Biophys J 72:5–17
8. Subramanian V, Shankaranarayanan C, Nair BU, Kanthimathi M, Manickkavachagam R, Ramasami T (1997) Chem Phys Lett 274:275–280
9. De Kerpel JO, Ryde U (1999) Proteins 36:157–174
10. Gray HB, Malmström BG (2000) J Biol Inorg Chem 5:551–559
11. Arcangeli C, Bizzarri AR, Cannistraro S (1999) Biophys Chem 78:247–257
12. Luise A, Falconi M, Desideri A (2000) Proteins 39:56–67
13. Arcangeli C, Bizzarri AR, Cannistraro S (2001) Biophys Chem 90:45–56
14. Romero C, Moratal JM, Donaire A (1998) FEBS Lett 440:93–98
15. De Beer S, Wittung-Stafshede P, Leckner J, Karlsson BG, Winkler JR, Gray HB, Malmström BG, Solomon EI, Hedman B, Hodgson KO (2000) Inorg Chim Acta 297:278–282
16. Swart M (2002) Density functional theory applied to copper proteins. PhD thesis, Rijksuniversiteit Groningen, Groningen
17. te Velde G, Bickelhaupt FM, Baerends EJ, Fonseca Guerra C, van Gisbergen SJA, Snijders JG, Ziegler T (2001) J Comput Chem 22:931–967
18. Swart M, van den Bosch M, Berendsen HJC, Canters GW, Mark AE, Snijders JG (2003) in preparation
19. Canters GW, Kalverda AP, Hoitink CW (1993) Structure and activity of type I Cu sites. In: Welch AJ, Chapman SK (eds) The chemistry of the copper and zinc triads. The Royal Society of Chemistry, Cambridge, pp 30–37
20. Pozdnyakova I, Guidry J, Wittung-Stafshede P (2000) J Am Chem Soc 122:6337–6338
21. Pozdnyakova I, Guidry J, Wittung-Stafshede P (2001) J Biol Inorg Chem 6:182–188
22. Berendsen HJC, van der Spoel D, van Drunen R (1995) Comput Phys Comm 91:43–56
23. Lindahl E, Hess B, van der Spoel D (2001) J Mol Mod 7:306–317
24. van Gunsteren WF, Billeter FR, Eising AA, Hünenberger PH, Krüger P, Mark AE, Scott WRP, Tironi IG (1996) Biomolec-

ular simulation: the GROMOS96 manual and user guide. Vdf Hochschulverlag AG an der ETH Zürich, Zürich
25. Berman HM, Westbrook J, Feng Z, Gilliland G, Bhat TN, Weissig H, Shindyalov IN, Bourne PE (2000) Nucleic Acids Res 28:235–242
26. Nar H, Messerschmidt A, Huber R, van de Kamp M, Canters GW (1991) J Mol Biol 218:427-447
27. Nar H, Messerschmidt A, Huber R, van de Kamp M, Canters GW (1991) J Mol Biol 221:765-772
28. Berendsen HJC, Postma JPM, van Gunsteren WF, Hermans J (1981) Interaction models for water in relation to protein hydration. In: Pullman B (ed) Intermolecular forces. Reidel, Dordrecht, pp 331–342
29. Hess B, Bekker H, Berendsen HJC, Fraaije JGEM (1997) J Comp Chem 18:1463–1472
30. Miyamoto S, Kollman PA (1992) J Comp Chem 13:952–962
31. Berendsen HJC, Postma JPM, Di Nola A, Haak JR (1984) J Chem Phys 81:3684–3690
32. Hol WGJ, van Duijnen PT, Berendsen HJC (1978) Nature 273:443–446
33. Matthews BW (1993) Curr Opin Struct Biol 3:589–593
34. Kalverda AP, Ubbink M, Gilardi G, Wijmenga SS, Crawford A, Jeuken LJC, Canters GW (1999) Biochemistry 38:12690–12697
35. Holm RH, Kennepohl P, Solomon EI (1996) Chem Rev 96:2239–2314
36. La Croix LB, Shadle SE, Wang Y, Averill BA, Hedman B, Hodgson KO, Solomon EI (1996) J Am Chem Soc 118:7755-7768
37. Guckert JA, Lowery MD, Solomon EI (1995) J Am Chem Soc 117:2817–2844
38. Gray HB, Malmström BG (1983) Comments Inorg Chem 2:203–209
39. Malmström BG (1994) Eur J Biochem 223:207–216
40. Williams RJP (1995) Eur J Biochem 234:363–381
41. Ryde U, Olsson MHM, Pierloot K, Roos BO (1996) J Mol Biol 261:586–596
42. Olsson MHM, Ryde U, Roos BO, Pierloot K (1998) J Biol Inorg Chem 3:109–125
43. Pierloot K, De Kerpel JO, Ryde U, Olsson MHM, Roos BO (1998) J Am Chem Soc 120:13156–13166
44. Ryde U, Olsson MHM (2001) Int J Quantum Chem 81:335–347
45. Swart M, van den Bosch M, Berendsen HJC, Canters GW, Snijders JG (2003) in preparation
46. Koradi R, Billeter M, Wüthrich K (1996) J Mol Graphics 14:51–55